

## Photo-rewritable material based on a metal oxide

Shin-ichi Ohkoshi,<sup>\*a</sup> Yoshihide Tsunobuchi,<sup>a</sup> Kazuhito Hashimoto,<sup>b</sup> Asuka Namai,<sup>a</sup> Fumiyoshi Hakoe,<sup>a</sup> and Hiroko Tokoro<sup>a</sup>

<sup>a</sup>Department of Chemistry, School of Science, The University of Tokyo, 7-3-1 Hongo, Bunkyo-ku, Tokyo 113-0033, JAPAN

<sup>b</sup>Department of Applied Chemistry, School of Engineering, The University of Tokyo, 7-3-1 Hongo, Bunkyo-ku, Tokyo 113-8656, JAPAN

### ABSTRACT

Photoinduced phase transition materials receive attention from both fundamental and technological viewpoints because they are used in high-density optical data storage. In this paper, we report a photoreversible phase transition at room temperature with a unique phase of  $\text{Ti}_3\text{O}_5$  (hereinafter, this new phase is called  $\lambda\text{-Ti}_3\text{O}_5$ ). The  $\lambda\text{-Ti}_3\text{O}_5$  phase, which is generated by a nanoscale size effect, is a metal conductor, and exhibits a photoinduced phase transition to  $\beta\text{-Ti}_3\text{O}_5$ , a semiconductor. The photoreverse process from  $\beta\text{-}$  to  $\lambda\text{-Ti}_3\text{O}_5$  is also observed. This phenomenon originates from a particular state of  $\lambda\text{-Ti}_3\text{O}_5$ , which is trapped at thermodynamically local energy minimum. Light irradiation causes the switching between this trapped state ( $\lambda\text{-Ti}_3\text{O}_5$ ) and the other energy minimum state ( $\beta\text{-Ti}_3\text{O}_5$ ).

**Keywords** Lambda-trititanium pentaoxide, Photoinduced metal-semiconductor phase transition

### INTRODUCTION

A phase-change optical disc technology was developed for practical application in 1980s, and resulted in the commercialization of digital versatile disc (DVD) in 1990s and Blu-ray<sup>®</sup> in 2000s<sup>1),2)</sup>. Currently, DVD and Blu-ray<sup>®</sup> use a chalcogen alloy (*e.g.*, GeSbTe) as an optical data storage material. Various materials, including photochromic compounds, donor-acceptor stacked molecules, spin crossover complexes, cyano-bridged metal assemblies, and perovskite manganites, have been studied as next-generation high-performance optical data storage<sup>3)</sup>. Herein we report a unique phase of titanium oxide,  $\lambda\text{-Ti}_3\text{O}_5$ , which meets the requirements for optical data storage memory. This material shows a reversible photoinduced metal-semiconductor phase transition between  $\lambda\text{-Ti}_3\text{O}_5$  and  $\beta\text{-Ti}_3\text{O}_5$  at room temperature. This is the first demonstration of a metal oxide with a photoinduced phase transition at room temperature<sup>4),5)</sup>.

### FORMATION AND CRYSTAL STRUCTURE OF $\lambda\text{-Ti}_3\text{O}_5$

A unique phase of a titanium oxide,  $\lambda\text{-Ti}_3\text{O}_5$ , was obtained as two types of morphologies through different synthetic methods: one of them is  $\lambda\text{-Ti}_3\text{O}_5$  nanocrystal in  $\text{SiO}_2$  matrix and the other is a flake form of  $\lambda\text{-Ti}_3\text{O}_5$  assembled by nanocrystals. The former is obtained by combining reverse-micelle and sol-gel techniques. The transmission electron microscope (TEM) image of  $\lambda\text{-Ti}_3\text{O}_5/\text{SiO}_2$  shows cubic-shape  $\text{Ti}_3\text{O}_5$  nanocrystals with a size of ca. 20 nm dispersed in a  $\text{SiO}_2$  matrix (Fig. 1a). Moreover, the X-ray diffraction (XRD) pattern indicates a crystal structure of  $C2/m$ , which crystal structure does not correspond to any reported crystal structures of  $\text{Ti}_3\text{O}_5$  ( $\alpha\text{-}$ ,  $\beta\text{-}$ ,  $\gamma\text{-}$ , and  $\delta\text{-}$ phases) (Fig. 2a).

Calcinating the anatase form of the  $\text{TiO}_2$  nanoparticles (size = 7 nm) under hydrogen at 1200 °C produces the flake form  $\lambda\text{-Ti}_3\text{O}_5$ , which is black (Fig. 1b). The TEM image shows that the flake (size =  $2 \pm 0.5 \mu\text{m}$ ) is assembled by  $25 \pm 15$  nm nanocrystals. The XRD pattern of the sample at room temperature corresponds to the aforementioned  $\lambda\text{-Ti}_3\text{O}_5$  in  $\text{SiO}_2$ , and the Rietveld analysis shows a monoclinic structure ( $C2/m$ ). Variable-temperature XRD measurements demonstrate that as the temperature increases, the diffraction peaks of  $\lambda\text{-Ti}_3\text{O}_5$  continuously change to  $\alpha\text{-Ti}_3\text{O}_5$  peaks with a crystal structure of  $Cmcm$ . Furthermore, heating the sample to 640 K and then cooling to 300 K causes  $\alpha\text{-Ti}_3\text{O}_5$  to return to  $\lambda\text{-Ti}_3\text{O}_5$ . Differential scanning calorimetry (DSC) measurements did not exhibit a meaningful peak, which differs vastly from the first-order phase transition between  $\beta\text{-Ti}_3\text{O}_5$  and  $\alpha\text{-Ti}_3\text{O}_5$  in a conventional large crystal  $\text{Ti}_3\text{O}_5$ . Hence, the phase transition between  $\lambda\text{-Ti}_3\text{O}_5$  and  $\alpha\text{-Ti}_3\text{O}_5$  is classified as a second-order type phase transition.

### MAGNETIC, ELECTRIC, AND OPTICAL PROPERTIES AND ELECTRONIC STRUCTURE OF $\lambda\text{-Ti}_3\text{O}_5$

Figure 3 shows the magnetic susceptibility ( $\chi$ ) versus temperature ( $T$ ) of the flake form  $\lambda\text{-Ti}_3\text{O}_5$  as well as the  $\chi$  versus  $T$  curve of a conventional large crystal  $\text{Ti}_3\text{O}_5$ .  $\lambda\text{-Ti}_3\text{O}_5$  has  $\chi$  values around  $2 \times 10^{-4}$  emu per Ti atom throughout the entire measured temperature region, suggesting that  $\lambda\text{-Ti}_3\text{O}_5$  is a Pauli paramagnet due to metallic conduction. Spin-orbital coupling on  $\text{Ti}^{3+}$  ion can explain the gradual decrease below 150 K, but small amount of Curie paramagnetism (ca. 0.1%), which may be due to defects in the material, is attributed to the rapid increase below 30 K. The  $\lambda\text{-Ti}_3\text{O}_5/\text{SiO}_2$  sample exhibits the same type of

$\chi$  versus  $T$  curve. The electric current versus voltage curve using atomic force microscopy in the contact mode has an electric conductivity ( $\sigma$ ) value of ca.  $3 \times 10^1 \text{ S cm}^{-1}$ , indicating that  $\lambda\text{-Ti}_3\text{O}_5$  is a near metallic conductor. Additionally, both the UV-vis and IR reflectance spectra indicate that  $\lambda\text{-Ti}_3\text{O}_5$  possesses metallic absorption over the ultraviolet and infrared wavelength regions. In contrast, the impedance measurement and reflectance spectra suggest that  $\beta\text{-Ti}_3\text{O}_5$  is a semiconductor with  $\sigma = 3 \times 10^{-2} \text{ S cm}^{-1}$  and a band gap of 0.14 eV.

The empirical relationship between the bond length and valence states gives estimated valence states for Ti(1), Ti(2), and Ti(3) in  $\lambda\text{-Ti}_3\text{O}_5$  of +3.37, +3.20, and +3.53, respectively. These valence states are close to  $\text{Ti}^{3\frac{1}{3}+}$ , indicating that  $\lambda\text{-Ti}_3\text{O}_5$  is a charge-delocalized system (Fig. 2a). This is consistent with  $\lambda\text{-Ti}_3\text{O}_5$  being a metallic conductor. The electronic structure of  $\lambda\text{-Ti}_3\text{O}_5$  is close to that of  $\alpha\text{-Ti}_3\text{O}_5$ . In contrast, the valence states of Ti(1), Ti(2), and Ti(3) in  $\beta\text{-Ti}_3\text{O}_5$  are +3.00, +3.79, and +3.32, respectively, which are close to the valence states for a charge-localized system of  $\text{Ti}^{3+} - \text{Ti}^{3\frac{2}{3}+} - \text{Ti}^{3\frac{1}{3}+}$  (Fig. 2b). The band structures of  $\beta\text{-Ti}_3\text{O}_5$  and  $\lambda\text{-Ti}_3\text{O}_5$  calculated by the first-principle calculation also supported these valence states.

## REVERSIBLE PHOTOINDUCED PHASE TRANSITION

When the flake form  $\lambda\text{-Ti}_3\text{O}_5$  is irradiated with 532 nm pulsed laser light (6 ns, 3 shots,  $1.5 \times 10^{-5} \text{ mJ } \mu\text{m}^{-2} \text{ pulse}^{-1}$ ) at room temperature, the irradiated area changes from black to brown (panels a and b in Fig. 4). Successively, irradiating with 410 nm continuous wave laser light ( $8 \times 10^{-3} \text{ mW } \mu\text{m}^{-2}$ ) causes the irradiated spots to return to black (panel c in Fig. 4). Alternatively irradiating with 532 nm and 410 nm lights repeatedly induces these color changes (panels d–f in Fig. 4). The XRD pattern shows that the brown area is assigned to the  $\beta$ -phase (monoclinic structure of  $C2/m$ ). Hence, the change from black to brown is due to the transition from the  $\lambda\text{-Ti}_3\text{O}_5$  to  $\beta\text{-Ti}_3\text{O}_5$ , whereas the converse is due to the transition from the  $\beta\text{-Ti}_3\text{O}_5$  to  $\lambda\text{-Ti}_3\text{O}_5$ . Furthermore, a similar phase transition is observed by irradiating with different pulsed-laser lights, 355 or 1064 nm.

To investigate the threshold value of laser power, a mixed sample of  $\lambda\text{-Ti}_3\text{O}_5$  and  $\beta\text{-Ti}_3\text{O}_5$  with ratio of 2 : 1 was irradiated with 532 nm pulsed laser light (one shot) at various laser power densities. The threshold laser power of  $\beta\text{-Ti}_3\text{O}_5 \rightarrow \lambda\text{-Ti}_3\text{O}_5$  is  $2.7 \times 10^{-6} \text{ mJ } \mu\text{m}^{-2}$ , and conversely, that of  $\lambda\text{-Ti}_3\text{O}_5 \rightarrow \beta\text{-Ti}_3\text{O}_5$  is  $1.0 \times 10^{-5} \text{ mJ } \mu\text{m}^{-2}$ . Such a threshold is important for recording storage media for long-lasting memory. The observed threshold values of the laser power densities used are the same order as laser power density used on DVD.

## THERMODYNAMIC INTERPRETATION OF THE PHOTOINDUCED PHASE TRANSITION

The thermodynamic analysis of  $\lambda\text{-Ti}_3\text{O}_5$  suggests that the present photoinduced metal-semiconductor phase transition is attributed to the phase transition from  $\lambda\text{-Ti}_3\text{O}_5$ , a metastable phase thermodynamically trapped at a local energy minimum state, to  $\beta\text{-Ti}_3\text{O}_5$ , a truly stable phase by irradiation (Fig. 5). Because metallic absorption allows  $\lambda\text{-Ti}_3\text{O}_5$  to effectively absorb light over a wide wavelength range from ultraviolet to near-IR, this metal-semiconductor phase transition can be observed by irradiating with 355, 532, and 1064 nm laser lights. The reverse photoinduced phase transition from  $\beta\text{-Ti}_3\text{O}_5$  to  $\lambda\text{-Ti}_3\text{O}_5$  is induced by the excitation from the valence band to the conduction band on  $\beta\text{-Ti}_3\text{O}_5$ , and then the excited state directly changes to  $\lambda\text{-Ti}_3\text{O}_5$  in the pulsed laser light irradiation experiment or thermally transits to  $\lambda\text{-Ti}_3\text{O}_5$  through  $\alpha\text{-Ti}_3\text{O}_5$  (*i.e.*,  $\beta \rightarrow \alpha \rightarrow \lambda\text{-Ti}_3\text{O}_5$ ) in the continuous wave laser light irradiation experiment.

## CONCLUSION

We reported a photoreversible metal-semiconductor phase transition at room temperature with a new phase of  $\text{Ti}_3\text{O}_5$ . This phenomenon originates from a particular state of  $\lambda\text{-Ti}_3\text{O}_5$  trapped at thermodynamic local energy minimum.  $\lambda\text{-Ti}_3\text{O}_5$  satisfies the operation conditions (operational temperature around room temperature, writing data by short wavelength near ultra-violet light for high memory density, and the appropriate threshold laser power to maintain long-term memory).

## ACKNOWLEDGEMENT

This work was performed under the management of the Project to Create Photocatalyst Industry for Recycling-oriented Society supported by NEDO. We are thankful for a Grant-in-Aid for the Global COE Program, from MEXT Japan.

## REFERENCES

1. N. Yamada, E. Ohno, K. Nishiuchi, N. Akahira, and M. Takao, *J. Appl. Phys.*, 69, 2849–2856 (1991).
2. M. Wuttig, and N. Yamada, *Nature Mater.*, 6, 824–832 (2007).
3. K. Nasu, *Relaxations of Excited States and Photo-Induced Structural Phase Transitions* (Springer, Berlin, 1997).
4. S. Ohkoshi, Y. Tsunobuchi, T. Matsuda, K. Hashimoto, A. Namai, F. Hakoe, and H. Tokoro, *Nature Chem.*, 2, 539–545 (2010).
5. *Nature Japan*, URL: <http://www.natureasia.com/japan/jobs/tokushu/detail.php?id=219>

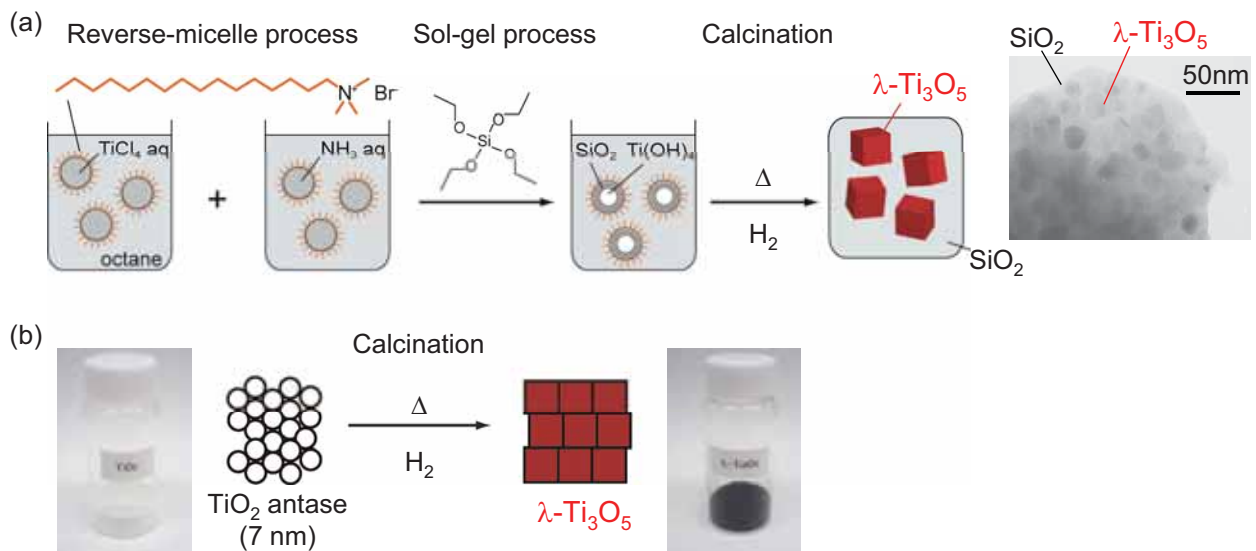


**Fig. 1** (a) Schematic illustration of the synthetic procedure of  $\lambda$ -Ti<sub>3</sub>O<sub>5</sub> nanocrystal in SiO<sub>2</sub> matrix using combination method between reverse-micelle and sol-gel techniques and TEM image of  $\lambda$ -Ti<sub>3</sub>O<sub>5</sub> nanocrystals in SiO<sub>2</sub> matrix. (b) Schematic illustration of the synthetic procedure of flake-form of  $\lambda$ -Ti<sub>3</sub>O<sub>5</sub>.

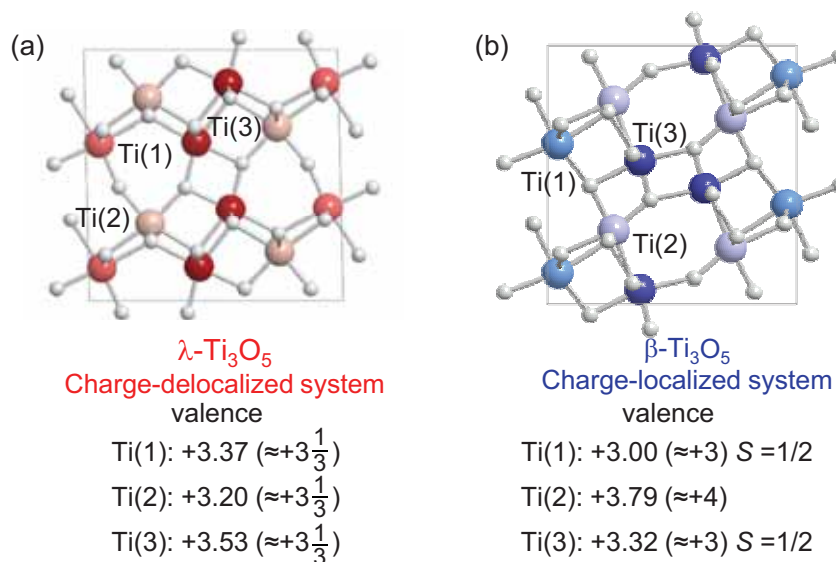


**Fig. 2** Crystal structures and valence states of (a)  $\lambda$ -Ti<sub>3</sub>O<sub>5</sub> and (b)  $\beta$ -Ti<sub>3</sub>O<sub>5</sub>.

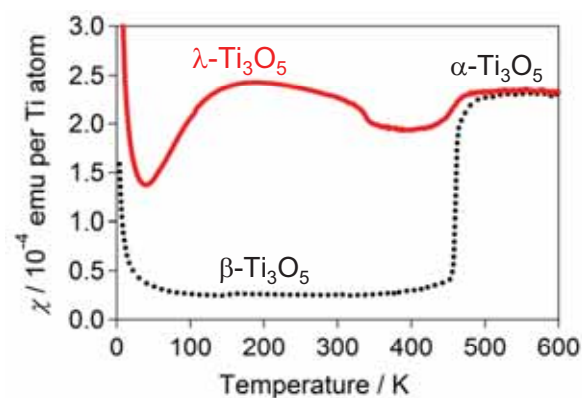


**Fig. 3**  $\chi$  versus  $T$  plots of flake-form of  $\lambda$ -Ti<sub>3</sub>O<sub>5</sub> (red line) and single crystal  $\beta$ -Ti<sub>3</sub>O<sub>5</sub> (black dotted line) under an external field of 0.5 T.

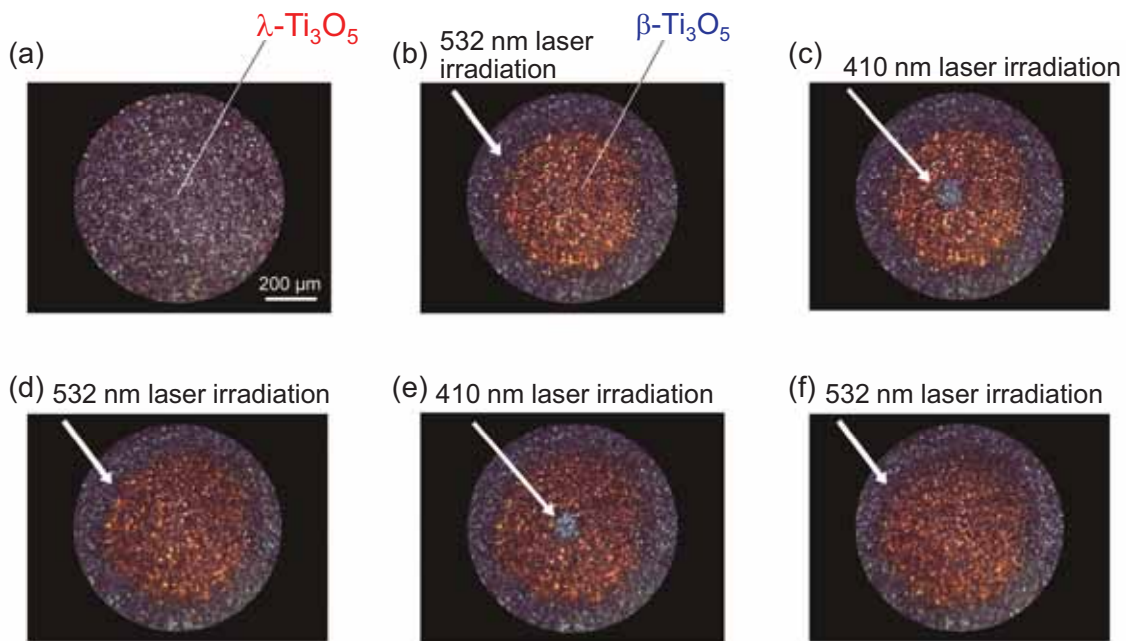


**Fig. 4** Reversible photoinduced phase transition in  $\lambda$ - $\text{Ti}_3\text{O}_5$ . Photographs of  $\lambda$ - $\text{Ti}_3\text{O}_5$  by the irradiation 532 nm pulsed laser and 410 nm continuous wave laser lights. When flake-form of  $\lambda$ - $\text{Ti}_3\text{O}_5$  was irradiated with 532 nm pulsed laser light at room temperature, the irradiated area changed from black (panel a) to brown (panel b). Successively, the spots returned to black upon irradiating with 410 nm continuous wave laser light (panel c). Photoinduced color changes were repeatedly observed by alternating 532 nm and 410 nm laser light irradiation (panels d-f).

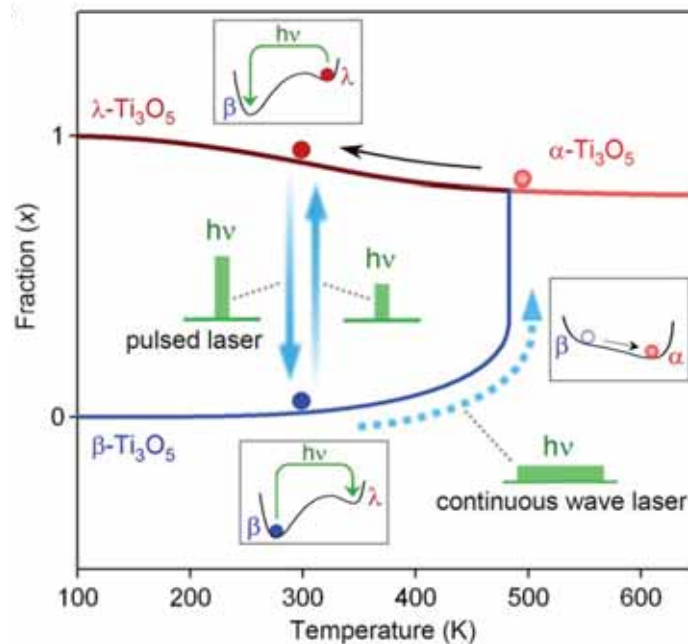


**Fig. 5** Mechanism of the photoinduced phase transition in  $\lambda$ - $\text{Ti}_3\text{O}_5$ . Schematic illustration of the pathways of the reversible photoinduced phase transition. Thermally populated phase versus temperature curves are described based on the  $G$  versus  $x$  plots for  $\text{Ti}_3\text{O}_5$  nanocrystals. Red, pink, and blue lines indicate  $\lambda$ - $\text{Ti}_3\text{O}_5$ ,  $\alpha$ - $\text{Ti}_3\text{O}_5$ , and  $\beta$ - $\text{Ti}_3\text{O}_5$ , respectively. The photoinduced phase transition from  $\lambda$ - $\text{Ti}_3\text{O}_5$  to  $\beta$ - $\text{Ti}_3\text{O}_5$  is attributed to the phase transition from a metastable phase to a true stable phase (downward blue arrow). In the reverse photoinduced phase transition from  $\beta$ - $\text{Ti}_3\text{O}_5$  to  $\lambda$ - $\text{Ti}_3\text{O}_5$ ,  $\beta$ - $\text{Ti}_3\text{O}_5$  directly transits to  $\lambda$ - $\text{Ti}_3\text{O}_5$  by the nanosecond (ns)-pulsed laser light irradiation (upward blue arrow), or thermally transits to  $\lambda$ - $\text{Ti}_3\text{O}_5$  through  $\alpha$ - $\text{Ti}_3\text{O}_5$  (*i.e.*,  $\beta$ -  $\rightarrow$   $\alpha$ -  $\rightarrow$   $\lambda$ - $\text{Ti}_3\text{O}_5$ ) by the continuous wave (cw) laser light irradiation (dotted blue arrow).